AIP | Review of Scientific Instruments

Highstability bimorph scanning tunneling microscope

B. L. Blackford, D. C. Dahn, and M. H. Jericho

Citation: Review of Scientific Instruments **58**, 1343 (1987); doi: 10.1063/1.1139658
View online: http://dx.doi.org/10.1063/1.1139658
View Table of Contents: http://scitation.aip.org/content/aip/journal/rsi/58/8?ver=pdfcov
Published by the AIP Publishing

High-stability bimorph scanning tunneling microscope

B. L. Blackford, D. C. Dahn, and M. H. Jericho

Department of Physics, Dalhousie University, Halifax, Nova Scotia, Canada B3H 3J5

(Received 14 January 1987; accepted for publication 27 April 1987)

A novel scanning tunneling microscope (STM) is described which is constructed almost entirely of aluminum and uses bimorph piezoelectric disks as the *x,y,z* drive elements. The design uses a simple, rugged tripod configuration for the fine motion drive arms. Coarse motion of the sample, which is mounted on an aluminum holder, is achieved by pushing or pulling, with a piezoelectric louse. Differential thermal expansion effects are avoided by design, to first order, and the resulting drift is $\leqslant 0.5$ Å/min after only a short warm-up period. It is easy to build and operate, and has good immunity to mechanical vibrations. The frequency response is flat to 5 kHz. The *x,y,z* drive sensitivity is 8 Å/V and the range is $\geqslant 12000$ Å. Some preliminary experimental results are presented, including atomic resolution images in air, of graphite and $NbSe_2$.

INTRODUCTION

The development of the scanning tunneling microscope (STM) by Binnig and Rohrer in 1983[1] has revolutionized the experimental study of surfaces. Atomic-resolution microscopy on a large class of materials, including insulators with the atomic force microscope (AFM),[2] is now possible. In contrast to conventional surface science techniques (such as the scanning electron microscope), which are very expensive and also lack atomic resolution, the STM is feasible in laboratories with limited financial resources. STMs have been developed in many laboratories around the world and several different STM designs have been reported. Many exciting results are appearing in the literature. See, for example, the review by Binnig and Rohrer.[3]

In our laboratory, we have designed, constructed, and successfully operated two different STMs.[4] Here we describe a novel design which uses three identical bimorph piezoelectric disks as the *x,y,z* translator (or drive) elements, respectively.[5] Three important features of a good STM design are (1) high mechanical stability, (2) low thermal drift, and (3) high scan rates. In our design, these features are achieved by making the STM almost exclusively of aluminum. Thermal drifts caused by using materials with different expansion coefficients are thereby greatly reduced.

I. DESIGN AND CONSTRUCTION

The operating principle of our STM is illustrated in the schematic view of Fig. 1 and a photograph of the entire unit is shown in Fig. 2. The main support block is machined from a single piece of aluminum. Its substantial thickness of 12 mm contributes to good mechanical stability and the high thermal conductivity of aluminum contributes to low thermal drift by reducing thermal gradients. The *x,y* scan and *z* fine positioning arms are constructed of lightweight Al tubing arranged in a rigid tripod configuration. The tunneling tip holder, the sample holder, and the baseplate for the coarse positioning louse (piezoelectric walking device) are also constructed of aluminum. The remaining possible sources of differential thermal expansion are then only the piezoelectric drive elements, the tunneling tip, and the sample. These are discussed below.

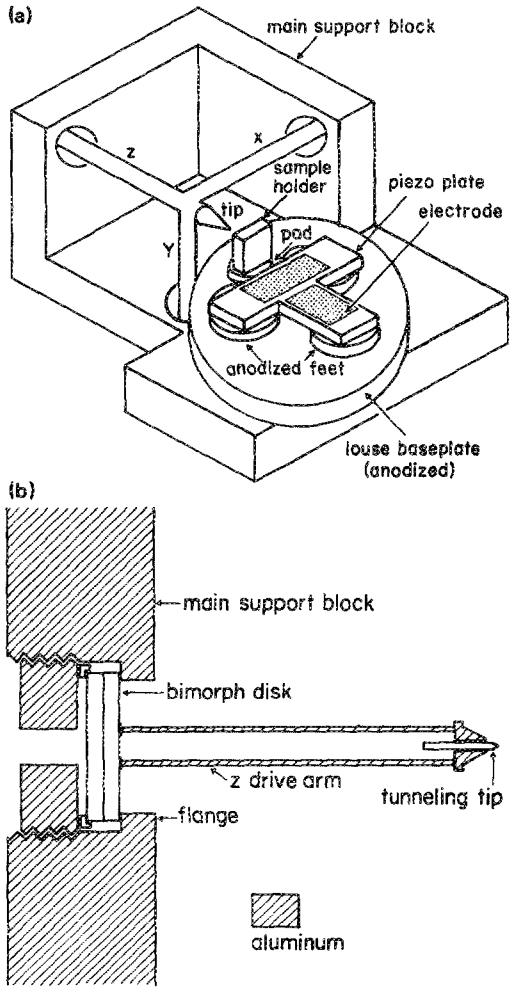

FIG. 1. (a) Schematic view of the STM. (b) Detail of the *z*-bimorph drive and tunneling tip.

 0034-6748/87/081343-06$01.30

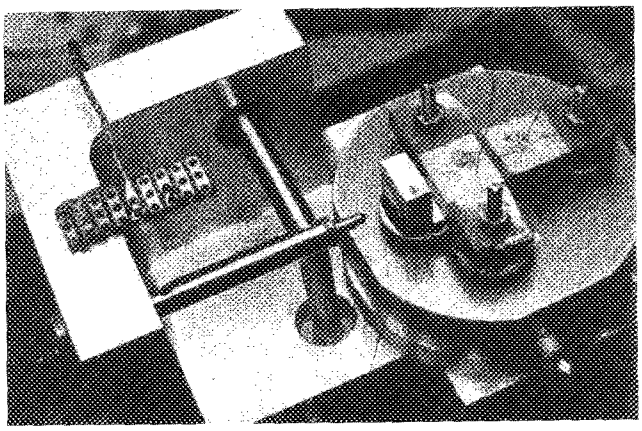

FIG. 2. Photograph of the complete STM unit.

A. *x*, *y*, *z* drive elements

In our STM, the piezoelectric drive elements for the *x*,*y*,*z* arms consist of three bimorph disks, one bonded to the end of each arm, as shown in Fig. 1(b). The bimorph disks are 2 mm thick $\times$ 14 mm in diameter and are made of Channel 5800 material.[6] The Al tube drive arms are bonded to the bimorph disks with Eccobond 285 epoxy,[7] whose thermal expansion is close to that of aluminum. The bimorph disks are housed in flanged holes drilled in the main support block and are held against the flange surface by a compressible gasket or spring. Longitudinal differential expansion between the bimorph disk and the block is accommodated by compression of the spring. In the radial direction, differential expansion of the disk is accommodated by slippage of the disk along the flange surface, rather than by buckling of the disk. The net result is that differential expansion of the bimorph disk does not move the drive arm with respect to the main support block of the STM, at least to first order. The holes housing the disks also serve to shield them electrically.

B. Tunneling tip

The tunneling tip was made from 0.5-mm-diam tungsten wire mounted in a conically shaped aluminum holder which screws into the end of the *z*-axis drive arm, as shown in Fig. 1(b). The wire rests firmly, but not tightly, in an insulating epoxy sleeve on the axis of the holder. The rigid connection between the wire and the holder is made by a local epoxy bond very near the tip. The short portion, <0.5 mm, of the wire beyond the epoxy is the only portion whose thermal expansion is of importance. The tungsten wire is electrically insulated from the drive arm by the epoxy. Electrical connection to the tungsten wire is made by a fine insulated wire running inside the drive arm. This arm also provides electrical shielding for the sensitive tunneling tip circuit.

C. Sample holder

The sample holder is mounted on an anodized Al pad, 12 mm in diameter by 5 mm in height, which can be electrostatically clamped to the louse baseplate independently of the louse feet [Fig. 1(b)]. The sample holder is electrically insulated from the Al pad by a thin layer of epoxy. The pad follows the motion of the louse in the *xz* plane but is only loosely coupled to it in the *y* direction. During a tunneling run the sample holder pad is clamped to the baseplate, while the louse feet are left free. This improves mechanical stability and eliminates thermal drifts caused by differential thermal expansion of the piezoelectric arms of the louse. Previous STMs which used a louse, mounted the sample either on the louse arms[1,8] or on one of the louse feet.[9]

D. Sample mounting

The sample is mounted on the vertical face of the sample holder. Thin samples can be glued directly to the front face of the holder. For thick samples it is better to drill a hole in the holder and mount the sample by its front face, thereby reducing differential thermal expansion effects due to the sample.

E. Coarse positioning

The louse used for coarse positioning of the sample holder was a hybrid of previous types.[1,8,9] It consists of a T-shaped piezoelectric plate (Channel 5400 material[6]) resting on three anodized Al feet through flexible ball-cone joints (Figs. 1 and 2). The surfaces of the feet and the baseplate were ground and polished by hand, using diamond abrasives in the size range 1–30 μm. Electrodes were formed on the piezo with conductive silver paint, which was also used to attach #40 copper lead wires. The electrodes defined two extension regions, one for *X* motion and one for *Z* motion. Step sizes were in the range of 100–1000 Å with voltages of 100–900 V applied to the arms of the T. Clamping voltages on the feet were typically 50 V.

F. Vibration isolation

Vibration isolation for our STM unit consists of several stages. First, the unit of Fig. 1 is mounted on top of five brass plates ($8\times15\times0.5$ cm) separated by Viton rubber spacers, similar to the pocket-size STM of Gerber *et al.*[10] (see Fig. 2). This combination is housed in a sheet metal box for electrical shielding. For operation in air, the metal box rests on a plywood plate ($25\times25\times4$ cm), a Pb plate ($25\times25\times2$), and another plywood plate ($37\times37\times2$). The latter rests on top of a 60-cm-high pier of twelve 20-kg sand bags piled on the floor of the laboratory. A plywood cover box (1 cm thick) over the whole system isolates against acoustic vibrations in the air. Vibrations propagating along the electrical leads are filtered out by successive mechanical coupling to a secondary plywood plate on the sand bags and to the brass plates immediately under the STM.

II. ELECTRONICS

As is usual in tunneling microscopy, the tip-to-sample spacing is controlled by a feedback system which drives the *z* piezo to keep the tunneling current constant. A block diagram of our STM circuit is shown in Fig. 3 and a detailed

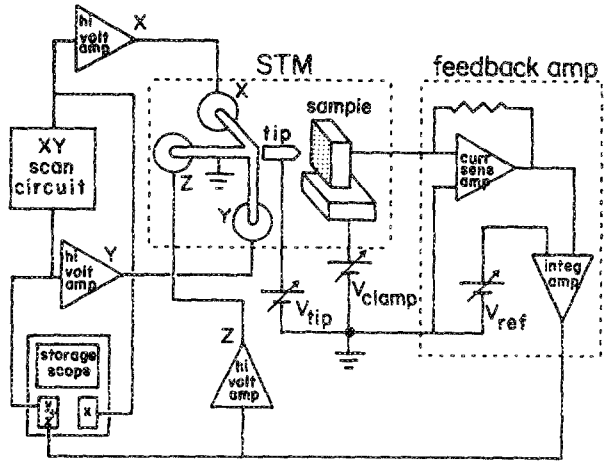

FIG. 3. Block diagram of the electronic circuitry for the STM.

schematic of the feedback amplifier is shown in Fig. 4. The tip is held at a fixed bias voltage V_{tip}. The sample is at virtual ground, being connected to the input of a current to voltage converter (IC1) with a sensitivity of 0.1 V/nA. The frequency response of the current measurement part of the circuit is limited by the open loop gain of IC1 at high frequencies. With a 1-MΩ tunnel junction impedance the bandwidth is about 2 kHz.

The output of IC1 is the input to an optional unity gain inverter (IC2) which is used to maintain negative feedback conditions when the tip bias is reversed. The logarithmic stage (IC3) improves the stability of the feedback system, although it is possible to operate without it. The next step is subtraction of an adjustable reference voltage (V_{ref}) which sets the tunneling current, followed by integration of the error signal. The output of the integrator drives the z piezo through a high-voltage amplifier with a gain of 100. A Trek model 601 and a homemade unit have both been used successfully.

This type of feedback system allows two different modes of imaging surface structures. We have successfully used

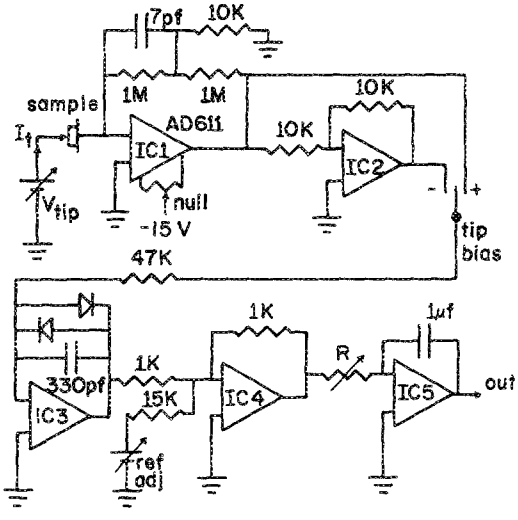

FIG. 4. Schematic diagram of the tip position-control feedback circuitry.

both the constant-current mode[1] and the higher speed variable-current mode.[11] In both imaging modes, the raster scan is generated as follows. The x piezo is driven by a high-voltage amplifier whose input is a triangle wave from a function generator. A synchronized square wave from the same generator is used to blank the display during the return trace. The square wave is also the input to a ramp circuit consisting of a 5-, 6-, 7-, or 8-bit binary counter and digital-to-analog converter which drives the y piezo through another high-voltage amplifier, thus incrementing y after every x scan.

The motion of the louse is controlled by applying properly sequenced voltages to the extension arms and the clampable feet. The voltages are turned on and off by FET switches, controlled by 5-V logic signals from a microcomputer. The maximum stepping rate was ~20 steps per second, which was limited by the computer used. The direction of motion can be reversed by software changes or by a hardware switch box which was installed between the FET switches and the louse.

III. PERFORMANCE

A. Long term stability

The STM described has been used in air to study the surface of a Au film deposited on mica, cleaved pyrolytic graphite, and $NbSe_2$. From the very first tunneling approach it was apparent that this STM design had good performance. Drift was never large and within 1 h, had settled down to 0.5 Å per minute or less. This has been confirmed by many subsequent tests ranging in duration from several minutes to 7 h. The same drift is expected for all three translator directions x,y,z, because of their identical design and construction (Fig. 1). The quoted drift is the apparent drift in the z direction, as determined by monitoring the feedback voltage on the z bimorph. This includes real z drift as well as drift in the x,y directions over sloping surfaces. The intrinsic drift value should, therefore, be even less than 0.5 Å per minute.

We found no evidence for the piezoelectric creep reported by Drake *et al.*[12] for a semicircular bimorph element, also made from Channel 5800 material. We suspect the difference is due to the method of mounting the bimorph. In their case it was simply resting on three supports, whereas ours was clamped all the way around the circumference [Fig. 1(b)].

B. Stability against vibrations

Our STM is quite insensitive to normal building vibrations and laboratory sounds. For example, in the constant-current mode, the feedback voltage on the z bimorph is not affected by slamming doors several meters away or by normal conversation at 1 m. Clapping hands immediately outside the wood cover box causes only minor changes. This is attributed to the rigid structure of the STM as well as to the vibration isolation system.

C. Frequency response and cross coupling

The frequency response of the STM was measured by applying an ac signal to one of the bimorph disks and detecting the output from either of the other bimorphs.[5] A lock-in amplifier was used as the detector, to get both amplitude and phase information. The response was flat, within 5%, for frequencies up to 5 kHz and the corresponding phase shifts were less than 15°. Weak resonances ($\times 2$) occurred at 7.2 and 10.6 kHz. Strong resonances ($\times 10$ to $\times 40$) occurred at 13, 14, 16, 20, 50, and 54 kHz. At higher frequencies the response decreased rapidly. The same results were obtained by exciting the x bimorph and detecting with the z bimorph, or vice versa. The conclusion is that our STM should be usable at scan rates up to 5 kHz, without signal degradation due to lack of mechanical fidelity.

The frequency response measurements also gave useful information about the cross coupling between bimorphs. An input signal of 3.5 V in one bimorph produced 5.6 mV in the other bimorphs, giving a cross-coupling coefficient of ~ 0.0016. This is less cross coupling than obtained with STMs using piezoelectric scan arms.[4] A cross-coupling coefficient was not given by Muralt *et al.*[5] for their bimorph STM. Cross coupling between the x and y scan arms has been suggested as an explanation for skewed atomic image patterns.[13] Low cross coupling is therefore desirable.

D. Calibration and range

The calibration factor, or sensitivity, of the bimorph drives is 8.0 ± 0.5 Å/V. This was determined from atomic images obtained on graphite and $NbSe_2$, operating the STM in air, and using the known lattice spacings. The applied voltages were typically less then 100 V. The rather large uncertainty is due to the skewed images and other distortions obtained, which may be intrinsic to the surfaces we studied. A calibration factor was obtained for both x and y drives and they agreed within the stated uncertainty. The calibration factor for the z drive is assumed to be the same as the others, because of its identical design. In fact, the z drive has been independently calibrated using a Michelson interferometer technique, giving 8 ± 0.5 Å/V in the range from -500 to $+500$ V.[14] One can safely apply ± 800 V to the bimorphs without concern for strain damage, therefore the maximum range is at least 12000 Å in each direction. The range can be increased further by using larger and/or thinner bimorph disks. These changes would however decrease the mechanical rigidity of the disks.

E. Examples of experimental results

Figure 5 shows a low resolution, topographic STM image in air, of a 1200-Å-thick gold film evaporated on a cleaved mica substrate. The mica substrate was cleaved in air prior to placement in the diffusion-pumped vacuum chamber. During pumpdown to a background pressure of 5×10^{-6} Torr, the substrate was exposed to glow discharge for 10 min at 0.1 Torr of air. The gold was evaporated from a resistance heated tungsten filament and deposited at a rate of ~ 10 Å per second.

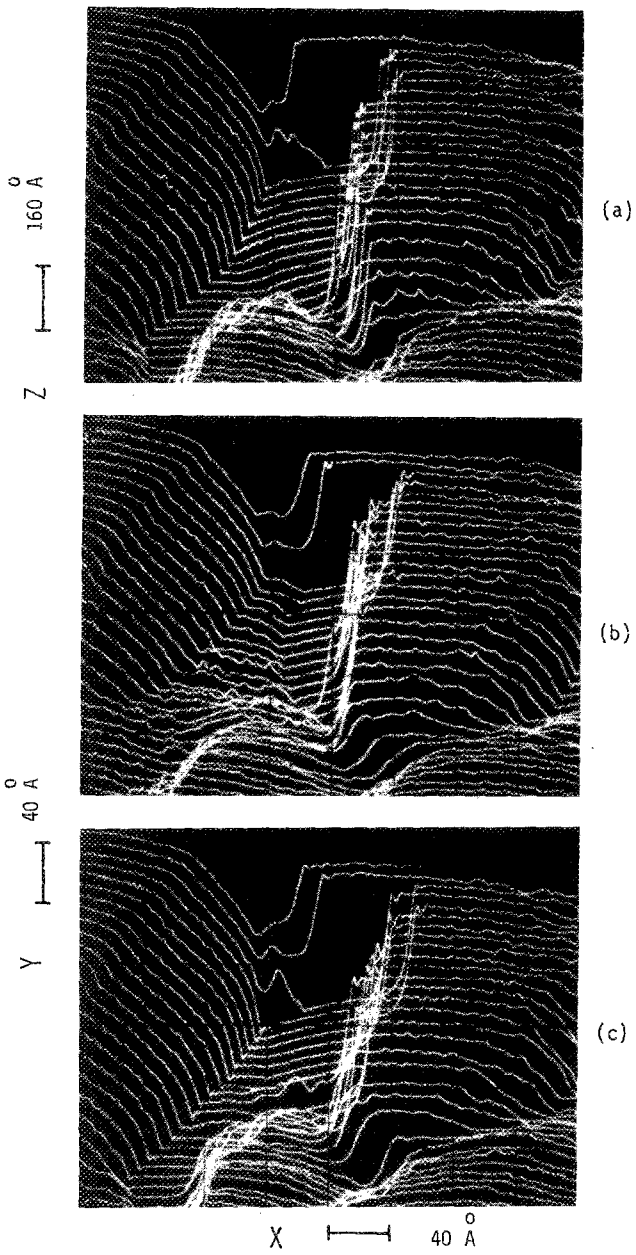

FIG. 5. Topographic STM images, in air, of a 1200-Å gold film on a cleaved mica substrate. x-scan frequency: 1 Hz. Scan direction: left to right and bottom to top. Tunneling current: 2 nA. Tip voltage: +180 mV. Biases on the x,y,z bimorph drives: 0, 0, 30 V, respectively. The images in (a), (b), and (c) were taken in the same location on the sample, at 4-min time intervals. Note the dynamic changes on the floor of the canyonlike feature, from (a) to (b) and (b) to (c).

The images in Fig. 5 are photographs taken from a storage oscilloscope screen, using the electronics in the constant-tunneling-current mode.[1] The surface texture in Fig. 5 is similar to that observed by others for Au (Ref. 12) and Ag (Ref. 15) films. It is characterized by broad hilly regions separated by steeper valleys, the so-called "island structure." The steep canyonlike structure in the center of the figure may, however, be the result of previously touching the surface with the probe tip.

Interesting dynamic changes were observed in the region of the canyon floor. These changes are depicted in the

sequential images of Figs. 5(a), 5(b), and 5(c) which were taken at 4-min intervals. (Each image required 30 s to produce.) In Fig. 5(a) the floor of the canyon is quite flat, while in Fig. 5(b) a prominent inclusion has appeared on the left-hand side of the canyon floor and extends all the way to the lower left corner of the figure. In Fig. 5(c) the inclusion has almost entirely disappeared and the image is essentially the same as in Fig. 5(a). In subsequent scans over the same area the image stayed like that of Fig. 5(c). The appearance of hillocks on gold has been reported by others[8] and attributed to the deposition of material from the tip to the sample. This could explain our case, but instabilities of the Au film or underlying mica are also possible explanations. Regardless of the explanation, it is a good example of the usefulness of a low drift STM for studying such phenomena. Note that the hill region in the upper left of Fig. 5 did not change noticeably during the entire sequence, which confirms the stability of the STM. The cliffs on the right of the figures are thought to be nonphysical as they are too steep for an STM to resolve and are probably due to tip switching.

Figures 6 and 7 show high resolution atomic STM images of cleaved pyrolytic graphite and $NbSe_2$, respectively, using the variable-tunneling-current mode described above. These images were obtained in air. The intensity modulation signal was sometimes high-pass filtered to remove frequency components near the scan frequency, caused by sloping surfaces. The frequency of the atomic signal depended on the number of atoms scanned, but was typically ten times higher than the scan frequency. The filtering produced better uniformity of the atomic images on the screen.

The hexagonal symmetry pattern expected for graphite and $NbSe_2$ is readily apparent in Figs. 6 and 7, respectively. However, we have observed skewed and/or distorted images in varying degrees. For an extreme example, in Fig. 7 the region on the right is greatly distorted compared to the central region. Note the differences between the two hexagons drawn on the figure. We believe that this may be a real distortion of the surface being imaged, since it is difficult to see how the STM could cause such localized distortions. Similar distortions have been reported recently by Smith *et al.*,[16] using the STM in a point contact mode where the tunneling resistance is as low as a few kilohms. They attribute the distortions to frictional forces between the tip and sample. It is possible that this could explain our distortions, although we were operating in the normal STM mode.

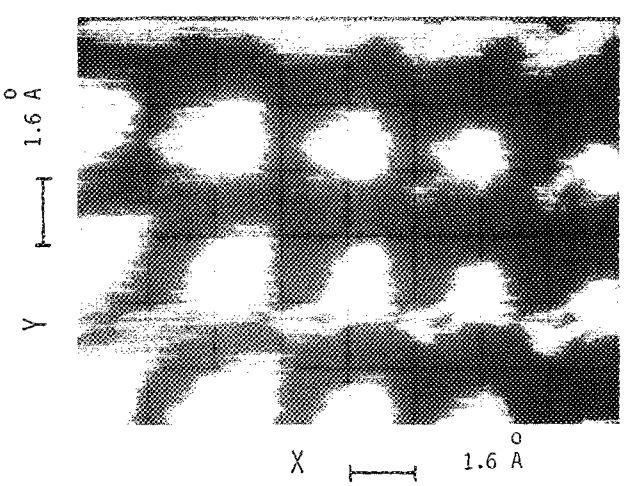

FIG. 6. High resolution atomic image in air and of pyrolytic graphite. x-scan frequency: 80 Hz. Tunneling current: 10 nA dc, with oscillations of ~4 nA p.p. due to the atoms. Tip voltage: +7 mV. The complete image was scanned and overwritten four times. x,y,z bias voltages: 0, 0, 107 V, respectively. No high-pass filtering.

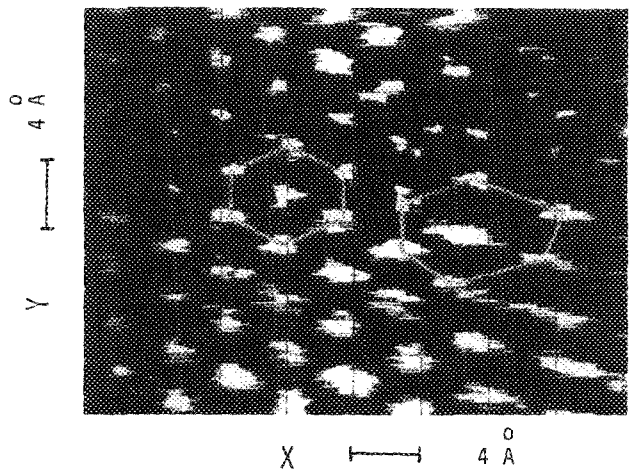

FIG. 7. High resolution atomic image, in air, of $NbSe_2$. x-scan frequency: 80 Hz. Tunneling current: 11 nA dc, with oscillations of ~5 nA p.p. due to the atoms. Tip voltage +9 mV. x,y,z bias voltages: 0, 40, −93 V, respectively. High-pass filter: 200 Hz.

Skewed images are a common feature of STM images reported by most investigators[11] and several explanations have been suggested. One explanation[3] attributes skew to thermal drift and/or piezoelectric creep. This cannot explain the skew in our images, since drift of our STM during the time (1.6 s) to obtain the atomic images would be negligible. In fact, the image of Fig. 6 was overwritten four times, which confirms the lack of drift. Another explanation[11] involves nonorthogonal motion of the x,y drives. This seems unlikely with the present STM design, considering the low cross-coupling coefficient discussed above, but is a possibility which needs further investigation.

ACKNOWLEDGMENTS

The authors wish to thank P. K. Hansma and J. K. Gimsewski for helpful discussions. We are also indebted to: J. Butler for electronics design and construction, particularly for the high voltage amplifiers which are not standard; and A. Feargrleve and R. Janc for the machining of the STM parts.

This work was partly supported by a grant from the Dalhousie University research development fund. One of us (DCD) was supported by a Killam post-doctoral fellowship and another (MHJ) was supported by a senior Killam research fellowship.

[1]G. Binnig and H. Rohrer, Surf. Sci. **126**, 236 (1983).
[2]G. Binnig, C. F. Quate, and C. Gerber, Phys. Rev. Lett. **56**, 930 (1986).

[3]G. Binnig and H. Rohrer, IBM J. Res. Develop. **30**, 355 (1986).
[4]M. H. Jericho, D. C. Dahn, and B. L. Blackford, Rev. Sci. Instrum. **58**, 1349 (1987).
[5]Our STM differs markedly from other bimorph designs, such as: P. Muralt, D. W. Pohl, and W. Denk, IBM J. Res. Develop. **30**, 443 (1986); U. Dürig, D. Pohl, and F. Rohner, IBM J. Res. Develop. **30**, 478 (1986).
[6]Channel Industries, Santa Barbara, CA.
[7]Emerson and Cuming Inc., Canton, MA.
[8]H. J. Mamin, D. W. Abraham, E. Ganz, and J. Clarke, Rev. Sci. Instrum. **56**, 2168 (1985); IBM J. Res. Develop. **30**, 492 (1986).
[9]G. F. A. van de Walle, J. W. Gerritsen, H. van Kempen, and P. Wyder, Rev. Sci. Instrum. **56**, 1573 (1985).
[10]C. Gerber, G. Binnig, H. Fuchs, O. Marti, and H. Rohrer, Rev. Sci. Instrum. **57**, 221 (1986).
[11]A. Bryant, D. P. E. Smith, and C. F. Quate, Appl. Phys. Lett. **48**, 832 (1986).
[12]B. Drake, R. Sonnenfeld, J. Schneir, P. K. Hansma, G. Slough, and R. V. Coleman, Rev. Sci. Instrum. **57**, 441 (1986).
[13]J. E. Demuth, R. J. Hamers, R. M. Tromp, and M. E. Welland, J. Vac. Sci. Technol. A **4**, 1320 (1986).
[14]R. McKenna, Honours Project, Dalhousie Univ., Physics Dept., 1987.
[15]J. K. Gimzewski, A. Humbert, J. G. Bednorz, and B. Reihl, Phys. Rev. Lett. **55**, 951 (1986).
[16]D. P. E. Smith, G. Binnig, and C. F. Quate, Appl. Phys. Lett. **49**, 1166 (1986).